22 February 1996

PHYSICS LETTERS B

ELSEVIER

Physics Letters B 369 (1996) 123–129

The Villain model on thin graphs

C.F. Baillie [a], N. Dorey [b], W. Janke [c], D.A. Johnston [d]

[a] *Computer Science Department, University of Colorado, Boulder, CO 80309, USA*

[b] *Department of Physics, University of Wales Swansea, Swansea, SA2 8PP, Wales, UK*

[c] *Institut für Physik, Johannes Gutenberg-Universität, D-55099 Mainz, Germany*

[d] *Department of Mathematics, Heriot-Watt University, Edinburgh, EH14 4AS, Scotland, UK*

Received 19 October 1995; revised manuscript received 21 November 1995

Editor: P.V. Landshoff

Abstract

We perform simulations of an absolute value version of the Villain model on ϕ^3 and ϕ^4 Feynman diagrams, "thin" 3-regular and 4-regular random graphs. The ϕ^4 results are in excellent quantitative agreement with the exact calculations by Dorey and Kurzepa for an annealed ensemble of thin graphs, in spite of simulating only a *single* graph of each size. We also derive exact results for an annealed ensemble of ϕ^3 graphs and again find excellent agreement with the numerical data for single ϕ^3 graphs. The simulations confirm the picture of a mean field vortex transition which is suggested by the analytical results. Further simulations on ϕ^5 and ϕ^6 graphs and of the standard XY model on ϕ^3 graphs confirm the universality of these results. The calculations of Dorey and Kurzepa were based on reinterpreting the large orders behaviour of the anharmonic oscillator in a statistical mechanical context so we also discuss briefly the interpretation of singularities in the large orders behaviour in other models as phase transitions.

1. Background and calculations

It has long been known that mean field behaviour is found in models with short range interactions living on tree-like structures such as Bethe lattices [1]. This approach circumvents some of the problems that appear with using infinite range interactions to get mean field results. Difficulties still arise, however, when dealing with the dominant boundary of such trees. Random graphs, which are locally tree-like and have no external legs, offer a way round this problem, giving a way of calculating and simulating models on closed lattices with short range interactions that still behave in a mean field like manner.

There has been a considerable amount of work on spin glass models on random graphs [2] mostly with Ising or Potts spins, often based on analogy with the corresponding Bethe lattice. Recently it was pointed out that transplanting methods from matrix models and 2D quantum gravity allowed a considerable simplification of many of the proofs that had been derived [3] and offered the possibility of attacking problems like replica symmetry breaking from a different perspective.

The matrix model inspired approach to discrete spin models was predated by independent work on the finite temperature quantum mechanics of the anharmonic oscillator, interpreted as a $d = 1$, $N = 1$ matrix model [4]. This described a Villain transcription of the continuous spin XY model on ϕ^4 graphs and gave a mean field vortex transition rather than the Kosterlitz-Thouless (KT) [5] transition of the standard two di-

SSDI 0370-2693(95)01526-4

mensional XY model. In essence, the thermodynamic limit of the ϕ^4 random graph model is described by large orders in the perturbation series of the anharmonic oscillator in finite temperature quantum mechanics.

If we write the finite temperature partition function for the anharmonic oscillator as

$$Z(\beta,g) = \int D\phi \exp\left(-\int_0^\beta d\tau(\tfrac{1}{2}\dot{\phi}^2 + \tfrac{1}{2}\phi^2 + g\phi^4)\right), \tag{1}$$

where $\beta = 1/T$ is the inverse temperature, and carry out the perturbative expansion in g,

$$Z(\beta,g) \simeq \sum_{k=0}^{\infty} Z_k(\beta) g^k, \tag{2}$$

then each $Z_k(\beta)$ may be written as a sum over Feynman diagrams, which is this case are random ϕ^4 graphs with k vertices, giving

$$Z_k(\beta) = (-1)^k \beta^k \sum_G S(G) \times \int_0^1 \cdots \int_0^1 \prod_{i=1}^{k} dt_i \prod_{\langle ij\rangle} \sum_{m_{ij}=-\infty}^{\infty} \exp(-|t_i - t_j + m_{ij}|). \tag{3}$$

In the above $S(G)$ is the symmetry factor, which will generically be unity for a large graph, the t_i are attached to each vertex [1], and the m_{ij} are attached to each link and summed over the integers. The partition function $Z_k(\beta)$ can be thought of as coming from embedding the ϕ^4 graph on a circle of period β. The finite temperature one-dimensional propagator that appears in the above,

$$D_{\langle ij\rangle} = \sum_{m_{ij}=-\infty}^{\infty} \exp(-|t_i - t_j + m_{ij}|), \tag{4}$$

assigns a time coordinate $t_{i,j}$ to each end of an edge as well as a winding number m_{ij} to the edge itself. Written in this form the similarity with the Villain version of the XY model [6], where the edge factor is

$$\tilde{D}_{\langle ij\rangle} = \sum_{m_{ij}=-\infty}^{\infty} \exp[-\tfrac{1}{2}\beta(\theta_i - \theta_j + 2\pi m_{ij})^2], \tag{5}$$

with θ taking values in the interval 0 to 2π, is apparent so we might expect the same sort of critical behaviour. We have, in effect, interpreted the finite temperature quantum mechanics of the anharmonic oscillator as an absolute value version of the Villain model living on thin random graphs.

As in [4] the free energy per vertex is defined as

$$F = -\lim_{k\to\infty} \frac{1}{k} \log\left|\frac{Z_k(\beta)}{n_k}\right|, \tag{6}$$

where n_k is the number of graphs of size k, $n_k \simeq (16)^k(k-1)!$. The energy per vertex in the model $\rho = \partial F/\partial\beta$ measures the expectation value of the target-space length of the embedded graph, and can be interpreted as a measure of the density of vortices in the model. The specific heat is also given by the standard formula $C = -\beta^2\partial^2 F/\partial\beta^2$, or equivalently by directly differentiating the energy $C = \partial\rho/\partial T$.

The analytical solution of the thin graph model proceeds by looking at the large orders behaviour of the anharmonic oscillator partition function [7] in Eq. (1). After a rescaling $x = 2\sqrt{-g}\phi$, the $k \to \infty$ saddle point solution is given by the trajectories of period β of a particle moving in the potential $V = -\frac{1}{2}x^2 + \frac{1}{4}x^4$. A non-trivial instanton solution only exists above a critical value of the period β (in the ϕ^4 case $\beta_c = \sqrt{2}\pi$). For $\beta < \beta_c$ the only contribution is from the trivial solution $x(t) \equiv x_{\min}$, where the particle sits at the bottom of the well. The change of behaviour at $\beta = \beta_c$ is taken as the signal for a phase transition in the associated absolute value Villain model. To obtain explicit expressions for the partition function we need to determine the dependence of the energy E associated with a given particle trajectory on the period β. This can be done by evaluating the first integral of the classical equations of motion,

$$\beta(E) = 2\int_{x_1}^{x_2} \frac{dx}{\sqrt{2[E - V(x)]}}, \tag{7}$$

where x_1 and x_2 are the turning points. In the ϕ^4 case, the above integral can be evaluated perturbatively

[1] We have performed a rescaling of t_i with respect to the conventions of [4] for convenience in the numerical simulations described later in the paper.

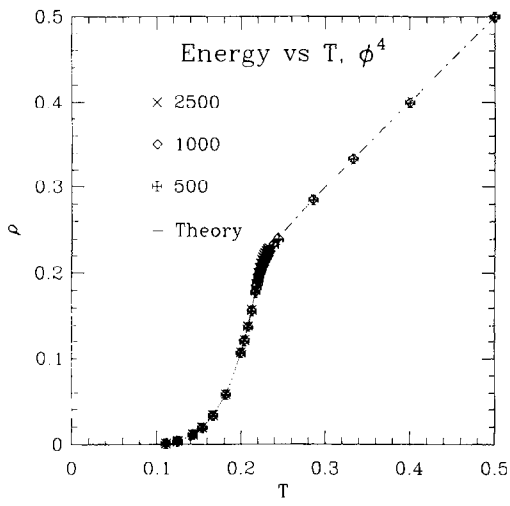

Fig. 1. The energy for various ϕ^4 graph sizes. A dotted line indicates the analytical prediction.

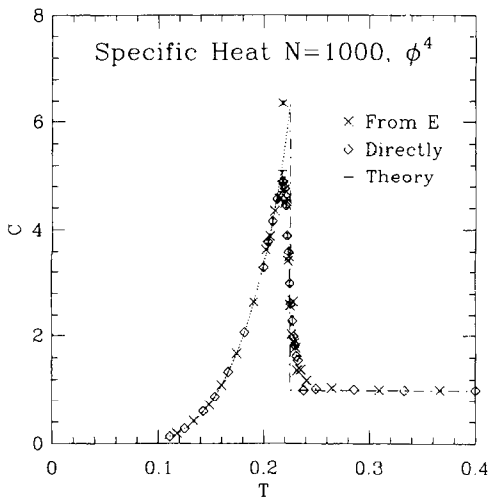

Fig. 2. The specific heat for a ϕ^4 graph of size 1000, obtained via both numerical differentiation of ρ and direct measurement. Again the dotted line represents the analytical curve.

near β_c [4]. Inverting the power series gives $E(\beta) = -\frac{1}{4} + 4(\beta - \beta_c)/(3\beta_c) + \ldots$. These solutions predict $\rho = 1/\beta$ for $\beta < \beta_c$ and $\rho \simeq \exp(-\beta)$ at large β. Similarly $C = 1$ for $\beta < \beta_c$ and sweeps up to a sharp cusp of height $\frac{19}{3}$ as $\beta \to \beta_c+$. In order to obtain the full temperature dependence of ρ and C shown in Figs. 1 and 2, we found it useful to express both $\beta(E)$ and the (scaled) classical action in terms of elliptic integrals, which can easily be evaluated with high precision. In summary, we see a second order transition of the mean-field type, with a sharp cusp discontinuity in the specific heat.

An explicit calculation can also be carried through in a similar style for the ϕ^3 case where the partition function is

$$Z(\beta, g) = \int D\phi \exp\left(- \int_0^\beta d\tau (\tfrac{1}{2}\dot{\phi}^2 + \tfrac{1}{2}\phi^2 + g\phi^3) \right) . \tag{8}$$

After a rescaling $x = -3g\phi$, the problem is mapped onto considering the trajectories of a particle in the potential $= -\frac{1}{2}x^2 + \frac{1}{3}x^3$. Evaluating the first integral of the classical equations of motion now gives

$$\beta(E) = 6^{1/3} \frac{2K(k)}{\sqrt{x_3 - x_1}} , \tag{9}$$

where K is the complete elliptic integral with modulus $k = \sqrt{(x_3 - x_2)/(x_3 - x_1)}$, and $x_1 < x_2 < x_3$ are the roots of $2[E - V(x)] = 2E + x^2 - 2x^3/3 = 0$. Inverting this gives $E(\beta) = -\frac{1}{6} + 6(\beta - \beta_c)/(5\beta_c) + \ldots$, where β_c is now 2π. The form of ρ and C are similar to the ϕ^4 graphs, but we now find a peak of $\frac{41}{10}$ in C as $\beta \to \beta_c+$ and $C = \frac{1}{2}$ for $\beta < \beta_c$. As in the ϕ^4 case, to compute the full temperature dependence of ρ and C, we first expressed the (scaled) classical action in terms of elliptic integrals,

$$I(\beta) = \tfrac{4}{15}\sqrt{\tfrac{2}{3}}(x_3 - x_1)^{5/2} \times [(2 - 2k^2 + 2k^4)E(k) - (2 - 3k^2 + k^4)K(k)] - E\beta . \tag{10}$$

Various numerical consequences of the analytical results are worth remarking upon as they are convenient for verifying that simulations are performing correctly. Firstly, we find that $\rho(T_c)$ is equal to T_c on ϕ^4 graphs. Secondly, it should be noted that the β_c is determined only by the period of oscillations around the minimum of the potential for *any* potential. Approximating this region with a quadratic gives $\beta_c = 2\pi/m$ if $V \simeq -V_0 + m^2(x - x_0)^2/2$, where x_0 is the minimum point. This reproduces the explicit results derived above for ϕ^3 and ϕ^4 graphs with rather less

pain. Finally, it is worth noting that, for a potential with an anharmonic term of the form $\phi^{2(p+1)}$, we will have $C = p$ for $T \geq T_c$ because $\rho = pT$ for $T \geq T_c$ in general.

We can contrast the critical behaviour described above with the standard XY model on a flat two dimensional lattice

$$Z = \prod_i \left[\int_0^{2\pi} d\theta_i \right] \exp\left(\beta \sum_{\langle ij \rangle} \cos(\theta_i - \theta_j) \right) , \quad (11)$$

which displays a topologically driven Kosterlitz-Thouless (KT) transition. The specific heat has only a broad cusp rather than a divergence. However, the correlation length has a critical singularity as does the spin susceptibility. In spite of the differences the physical picture of the transition on thin graphs is still very similar to that of the standard KT transition. Given the interpretation of ρ as a vortex density, the preceding saddle point results show that as the temperature is increased (ie β is decreased) vortices are liberated, with the vortex density increasing by almost an order of magnitude around β_c.

It is not a foregone conclusion that putting the model on *any* collection of random graphs will give mean field behaviour – the model still displays a KT transition on an annealed set of planar random graphs (ie when coupled to 2D quantum gravity). An explicit check in simulations of the thin graph predictions is therefore not totally vacuous. We have another motivation in carrying out simulations: the work in [3] revealed, surprisingly, that calculations made for the Ising model on an annealed ensemble of thin graphs were in excellent quantitative agreement with simulations on a *single* graph. There is thus self-averaging for the Ising ferromagnetic transition on such graphs. We shall check the self-averaging for the XY transition in the simulations reported in the next section, in which we look at the absolute value Villain action on ϕ^3, ϕ^4, ϕ^5 and ϕ^6 random graphs. We also simulated the standard XY action on ϕ^3 graphs to check it the universality of our results.

2. Simulations

We need to exercise a little care in defining our observables in the simulation because of the unusual form of the Boltzmann factors in the partition function [8]. If we define the auxiliary sums

$$\Sigma_0 = \sum_{m_{ij}=-\infty}^{\infty} \exp(-\beta|t_i - t_j + m_{ij}|) ,$$

$$\Sigma_1 = \sum_{m_{ij}=-\infty}^{\infty} |t_i - t_j + m_{ij}| \exp(-\beta|t_i - t_j + m_{ij}|) ,$$

$$\Sigma_2 = \sum_{m_{ij}=-\infty}^{\infty} |t_i - t_j + m_{ij}|^2 \exp(-\beta|t_i - t_j + m_{ij}|) , \quad (12)$$

then the definition of the energy $\rho = \partial F/\partial\beta$ applied to the partition function in Eq. (3) gives

$$\rho = \frac{1}{k} \left\langle \sum_{\langle ij \rangle} \frac{\Sigma_1}{\Sigma_0} \right\rangle - \frac{1}{\beta} \quad (13)$$

for the energy per site, where the $\langle\ \rangle$ denote a thermal average and the additional $1/\beta$ comes from the overall factor of β^k that appears when the t_i are rescaled.

The specific heat can be obtained in the simulations either by direct numerical differentiation of the measurements of ρ using $C = \partial\rho/\partial T$, or by differentiating Eq. (3) twice to give

$$C = \beta^2 k \left(\langle \rho^2 \rangle - \langle \rho \rangle^2 \right) + \frac{\beta^2}{k} \left\langle \sum_{\langle ij \rangle} \left(\frac{\Sigma_2}{\Sigma_0} - \frac{\Sigma_1^2}{\Sigma_0^2} \right) \right\rangle - 1 . \quad (14)$$

The second term is non-canonical and is due to the summed Boltzmann factors whereas the -1 results from the overall β^k.

Having decided on our observables, it now remains to choose an update scheme for the simulation. A simple Metropolis update can be used quite efficiently by adopting a discrete approximation to the periodic t_i and then tabling the resulting Boltzmann factors and associated sums $\Sigma_{0,1,2}$, which can then be looked up during the course of the simulation [8]. Depending on the temperature, we took from 100 to 1000 different t values for the tables, which were constructed by truncating the sum over m_{ij} at ± 100. Increasing these limits made no appreciable difference to the measured results in any of the simulations reported here. In doing this we are taking a $Z_{100} \ldots Z_{1000}$ approximation

to the $O(2)$ symmetry of the model. Notice that for the absolute value version of the Villain model one has to be quite careful with this approximation, in particular at low temperatures, since the associated discretization error enters linearly in the action and not squared as in the standard Villain model. It is perhaps worth remarking that one could equally well envisage leaving the m_{ij} as free variables on each link to be sampled in the course of the simulation, but previous work in which the sum is carried out *a priori* as here has given good results for the standard Villain/XY model [8] and we stick to this.

The final ingredient in the simulations is the choice of a random graph. The calculations we have outlined in the first section are supposedly for an annealed ensemble of thin graphs, so in theory we should carry out "flip" moves in the same fashion as in simulations of 2D gravity on planar graphs. However, as we are interested in checking the self-averaging properties of the graphs we take a *single* graph of each size to compare with the calculations[2].

We simulated the absolute value Villain model of Eq. (3) on ϕ^3 and ϕ^4 graphs of size up to 2500 vertices, as well as small runs of $N = 250$ ϕ^5 and ϕ^6 graphs. In all the cases we carried out 500000 Metropolis sweeps at each β value, with a measurement every tenth sweep, after allowing a suitable amount of equilibration time. As we have indicated *no* flip moves were carried out on the graphs concerned. The energy and specific heat, defined as above, were the principal observables. In addition, we also simulated the standard XY model of Eq. (11) on ϕ^3 graphs, using a single cluster update, largely as a check on the universality of the Villain model results.

Turning now to the results themselves we can see in Fig. 1 that the energy matches closely the predictions of [4]. There is a low temperature exponential growth with a "knee" at the phase transition $T = 1/\sqrt{2}\pi$ ($\simeq$ 0.225) followed by linear growth at larger T. It is also clear from Fig. 1 that $\rho(T_c) = T_c$, as predicted by the analysis in the previous section. We can obtain the specific heat either from direct differentiation of the energy or by measuring the observable defined in Eq. (14), and both are plotted in Fig. 2 for a graph of size 1000. This is the smallest graph size at which the peak reaches its expected value ($\frac{19}{3}$) – larger graphs give similar results, whereas the peak is appreciable lower and more rounded on the smaller graphs simulated.

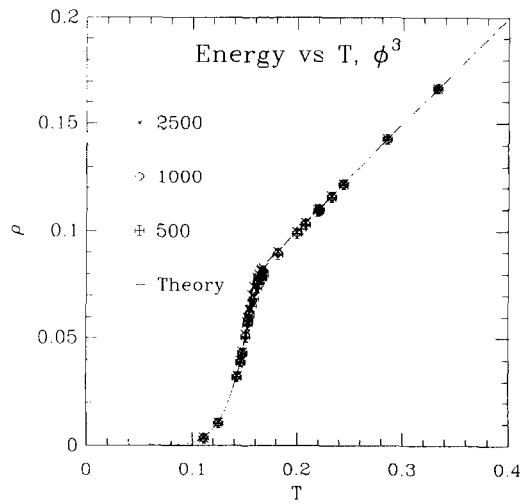

Fig. 3. The energy for various ϕ^3 graph sizes. The dotted line indicates the analytical prediction.

Fortified by the good agreement between the analytical and numerical results for ϕ^4 graphs we can move on to look at the possible variations on the theme that were outlined in the introduction. We consider the ϕ^3 graphs first. In Fig. 3 we plot the energy for various graph sizes, showing clearly the similarity with the ϕ^4 results. The "knee" in the curve is at the expected value of $T_c = 1/2\pi \simeq 0.16$. The specific heat curve obtained by numerical differentiation of these results is shown in Fig. 4 and is clearly of the same form as the ϕ^4 curve in Fig. 2, with the correct large T limit of $\frac{1}{2}$.

We have not carried out such extensive simulations of the ϕ^5 and ϕ^6 random graphs, simply contenting ourselves with verifying that the general form of the energy is similar and that the large T limit is correct. In Fig. 5 the energy is plotted up to very large T for ϕ^3, ϕ^4, ϕ^5 and ϕ^6 graphs of size 250. From the slopes it is clear that the specific heat prediction $C \rightarrow p$ for $T \rightarrow \infty$ on $\phi^{2(p+1)}$ graphs is satisfied to a high degree of accuracy. The finite size effects for a given graph size increase with the degree of the vertices, which

[2] It should be noted that a (quenched) average over graphs becomes essential when non-self-averaging transitions such as those in spin glasses are simulated, so it is not always possible to avoid the onerous task of simulating an ensemble of different graphs.

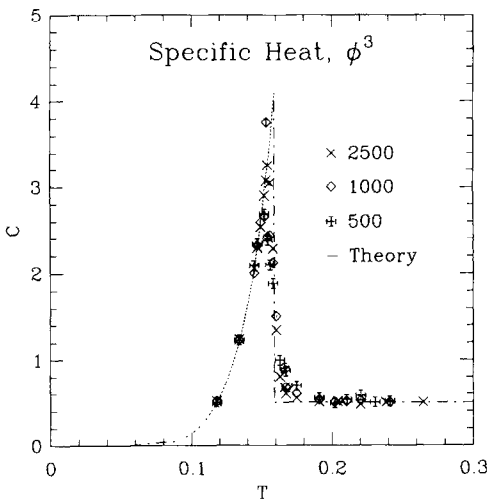

Fig. 4. The specific heat for ϕ^3 graphs of various sizes, obtained via numerical differentiation of ρ. The dotted line shows the analytical prediction.

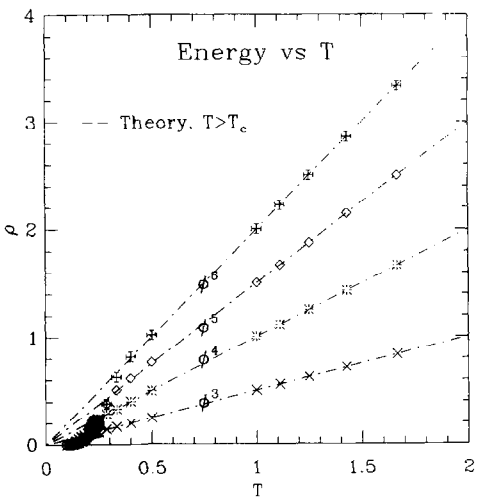

Fig. 5. The energy for ϕ^3, ϕ^4, ϕ^5 and ϕ^6 graphs. The linear prediction, $\rho = pT$ on $\phi^{2(p+1)}$ graphs when $T \geq T_c$, is shown as dotted lines to emphasize the very good fit.

agrees with the intuitive picture of $\phi^{2(p+1)}$ graphs being more "tree-like" for smaller p with a given number of vertices.

We would expect that the standard XY model with cosine action would still give us similar results on grounds of universality, but as we have no analytical calculations to fall back on in this case it is worthwhile verifying this explicitly with simulations. We therefore simulated the standard XY model on ϕ^3 graphs of various sizes, with similar statistics to the Villain model simulations but using a single cluster update for improved efficiency. The specific heat, measured directly in the simulation, is plotted in Fig. 6 for various lattice sizes, where it is clear that, although the small and large T limits are different from the Villain models ($\frac{1}{2}$ and 0 respectively), there is still a sharp cusp in the curve. This would again indicate a transition of mean field rather than KT type, where there is a much gentler bump in the specific heat curve away from the phase transition point. As for the standard Villain model [9], the differences can be understood by an approximate mapping of the absolute value version of the Villain model onto the cosine model. By adapting the formulas in [9] to the present case, we find that the temperature scales should be related by $I_1(\beta^{\cos})/I_0(\beta^{\cos}) = (\beta/2\pi)^2/\left(1 + (\beta/2\pi)^2\right)$, where $I_{0,1}$ are Bessel functions and $\beta^{\cos}$ denotes the inverse temperature of the cosine model. Inserting $\beta_c = 2\pi$ this predicts $I_1(\beta_c^{\cos})/I_0(\beta_c^{\cos}) = \frac{1}{2}$ or $T_c^{\cos} = 0.8625\ldots$, in good agreement with the peak location observed in Fig. 6.

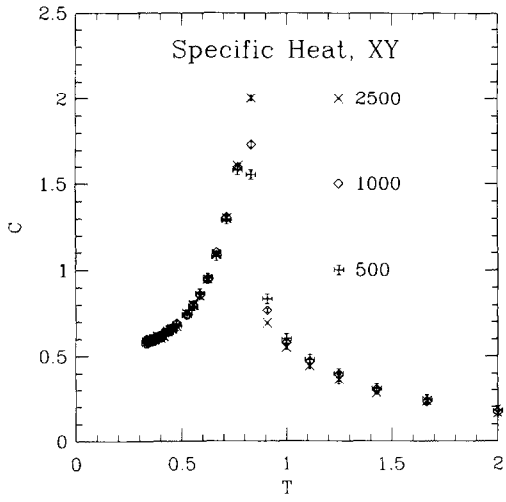

Fig. 6. The specific heat for the *standard XY* model on ϕ^3 graphs of various sizes.

3. Conclusions and other models

The saddle point predictions for the energy and specific heat of the absolute value Villain model on various random graphs are verified by the simulations we

have carried out. As one might expect the standard XY model on "thin" ϕ^3 graphs behaves in an analogous fashion, with a mean-field-like transition rather than a KT transition. The second point worth emphasizing is that we have not needed to simulate an annealed ensemble of random graphs to get good *quantitative* agreement with the theory, just as for the Ising ferromagnet on thin graphs [3]. This should be contrasted with the planar graphs in 2D gravity where an annealed sum, usually implemented by flip moves in a simulation, appears to be essential. Such self-averaging means that, unless one is very unlucky, any large thin graph is as good as another.

We are not restricted to the simple anharmonic oscillator in searching for statistical mechanical interpretations of large orders behaviour in quantum mechanics. Another example was considered by one of the authors of this paper in [10], namely the quantum mechanics of an anisotropic anharmonic oscillator, where the partition function is

$$Z = \int D\phi_1 D\phi_2 \exp\Big(- \int_0^\beta d\tau [\tfrac{1}{2}(\dot\phi_1^2 + \dot\phi_2^2 + \phi_1^2 + \phi_2^2) + g(\phi_1^4 + 2c\phi_1^2\phi_2^2 + \phi_2^4)] \Big) . \tag{15}$$

Taking c as the control parameter rather than β, the large orders behaviour shows a singularity at $c = 1$, where the model is rotationally symmetric. For $-1 \le c < 1$ the quartic $\phi_1^4 + \phi_2^4$ terms dominate and the instanton solution is $\phi_1(t) = u(t), \phi_2(t) = 0$, where

$$u(t) = \sqrt{\frac{1}{2}} \frac{1}{\cosh(t - t_0)} , \tag{16}$$

whereas for $c > 1$ the $\phi_1^2\phi_2^2$ term dominates and the solution is of the form $\phi_1(t) = \phi_2(t) = u(t)/\sqrt{2}$. Looking at the Feynman diagrams generated by the model we can see that it is a sort of loop gas, with ϕ_1 loops and ϕ_2 loops mixing via the $\phi_1^2\phi_2^2$ vertex and a propagator $D_{\langle ij \rangle}$ between the individual vertices on loops of both types. If we consider a ratio of mixed to pure vertices,

$$M = 1 - \frac{2\phi_1^2}{\phi_1^4 + \phi_2^4} \tag{17}$$

we can see that random graphs are filled with ϕ_1 loops only for $-1 \le c < 1$ ($M = 1$) and an even mixture of ϕ_1 and ϕ_2 loops for $c > 1$ ($M = 0$). The singular behaviour at $c = 1$ can thus be viewed as a sort of magnetization transition. It would be an interesting exercise to see if other large orders results in quantum mechanics could be cast in a statistical mechanical mould.

Acknowledgements

C.F.B. is supported by DOE under contract DE-FG02-91ER40672 and by NSF Grand Challenge Applications Group Grant ASC-9217394. N.D. is supported by a PPARC advanced fellowship. W.J. thanks the Deutsche Forschungsgemeinschaft for a Heisenberg fellowship. This work has been carried out in the framework of the EC HCM network grant ERB-CHRX-CT930343.

References

[1] H.A. Bethe, Proc. R. Soc. A 150 (1935) 552;
C. Domb, Adv. Phys. 9 (1960) 145;
T.P. Eggarter, Phys. Rev. B 9 (1974) 2989;
E. Müller-Hartmann and J. Zittartz, Phys. Rev. Lett. 33 (1974) 893.

[2] M. Mezard and G. Parisi, Europhys. Lett. 3 (1987) 1067;
I. Kanter and H. Sompolinsky, Phys. Rev. Lett. 58 (1987) 164;
K. Wong and D. Sherrington, J. Phys. A 20 (1987) L793; A 21 (1988) L459;
C. de Dominicis and Y. Goldschmidt, J. Phys. A 22 (1989) L775; Phys. Rev. B 41 (1990) 2184;
P.-Y. Lai and Y. Goldschmidt, J. Phys. A 23 (1990) 399.

[3] C. Bachas, C. de Calan and P. Petropoulos, J. Phys. A 27 (1994) 6121;
C. Baillie, D.A. Johnston and J.-P. Kownacki, Nucl. Phys. B 432 (1994) 551;
C. Baillie, W. Janke, D.A. Johnston and P. Plechac, Nucl. Phys. B 450 (1995) 730.

[4] N. Dorey and P. Kurzepa, Phys. Lett. B 295 (1992) 51.

[5] J.M. Kosterlitz and D.J. Thouless, J. Phys. C 6 (1973) 1181;
J.M. Kosterlitz, J. Phys. C 7 (1974) 1046;
V.L. Berezinski, JETP 34 (1972) 610.

[6] J. Villain, J. Phys. (Paris) 36 (1975) 581.

[7] J. Le Guillou and J. Zinn-Justin, eds., Large Order Behaviour of Perturbation Theory (North-Holland, Amsterdam, 1989).

[8] W. Janke and K. Nather, Phys. Lett. A 157 (1991) 11; Phys. Rev. B 48 (1993) 7419.

[9] W. Janke and H. Kleinert, Nucl. Phys. B 270 [FS 16] (1986) 135.

[10] W. Janke, Phys. Lett. A 143 (1990) 107.